

Analysis of Dynamic Properties of Forest Beetle Outbreak Model

Xuetian Zhang¹ and Chunrui Zhang^{1,†}

Abstract This paper mainly studies the dynamic properties of the forest beetle outbreak model. The existence of the positive equilibrium point and the local stability of the positive equilibrium point of the system are analyzed, and the relevant conclusions are drawn. After that, the existence of Turing instability, Hopf bifurcation and Turing-Hopf bifurcation are discussed respectively, and the necessary conditions for existence are given. Finally, the normal form of the Turing-Hopf point is calculated, and some dynamic properties at the point are analyzed by numerical simulation.

Keywords Reaction-diffusion equation, Turing instability, Hopf bifurcation, Turing-Hopf bifurcation

MSC(2010) 34C23, 35K57.

1. Introduction

Disturbance is defined as any relatively discrete event that disrupts ecosystem, community or population structure in time and alters resources, substrate availability or physical environment [13]. Forest disturbance is considered to be a key factor affecting terrestrial biological and geochemical processes, and it is closely related not only to pests and diseases but also to forest fires. For this reason, many scholars have conducted many studies on the relationship between forests, beetles and forest fires.

Forest fires and pests are two natural disturbances to forests, and they have had a devastating impact on the succession of forests. Forest fires not only burn down forests and reduce its stand density, but also destroy forest structures and reduce the use value of forests. Forest fires kill seedlings and saplings, therefore prolong the forest regeneration period. The topsoil and rocks of the burned forest land are exposed, and many places become barren mountains and ridges, making it difficult for the forest to recover. According to statistics, an average of 100,000 square kilometers of forests in China are infested with pests and diseases every year. If it continues to develop, the shelterbelt project that involves half of the country's safety will be in danger of being destroyed by the pests population. In order to minimize the damage caused by pests and forest fires to the forest and to better carry out the forest management and control, many experts and scholars have established various pine beetle models for different environments and studied

[†]The corresponding author.

Email address: xuetianmath@163.com (X. Zhang), math@nefu.edu.cn (C. Zhang)

¹Department of Mathematics, Northeast Forestry University, Harbin, Heilongjiang 150040, China

them (see [1–3, 7–9, 14, 15, 18–20, 26]). In [3], Chen proposed a mathematical model for beetle outbreaks as a single perturbation in forest population dynamics or in combination with wildfire perturbations:

$$\begin{cases} \frac{dV}{dt} = r_v V \left(1 - \frac{V}{K_v} - f_k \frac{B}{r+B} \right), \\ \frac{dB}{dt} = r_b B \left(1 - \frac{B}{K_e} \right) - \frac{\alpha B^2}{1+\beta B^2}, \end{cases} \tag{1.1}$$

where V and B represent the number of pine trees and the number of beetles at time t respectively. r_v and K_v are the natural growth rate and the carrying capacity of pine trees respectively. f_k represents the percentage of successfully attacked pines which are killed. r represents the threshold for the number of successfully attacked beetles. r_b and K_e are the natural growth rate and the carrying capacity of beetles respectively. α is the pine defense rate. β is the inverse of the beetle density, when the pine defense is saturated. All parameters involved with the model are positive.

Based on model (1.1), Chen proposed model (1.2) with forest fire disturbance as follows:

$$\begin{cases} \frac{dV}{dt} = r_v V \left(1 - \frac{V}{K_v} - f_k \frac{B}{r+B} \right) - P \frac{V}{K_v} M_v V, \\ \frac{dB}{dt} = r_b B \left(1 - \frac{B}{K_e} \right) - \frac{\alpha(1-cM_v)B^2}{1+\beta B^2} - M_b P \frac{V}{K_v} M_v B, \end{cases} \tag{1.2}$$

where M_v and M_b represent the impact intensity of a forest fire on trees and beetles, respectively. P represents the probability of a forest fire, and c is the parameter of fire weakening the pine tree’s defense against beetles. M_v , M_b , P and c are positive parameters.

Since Lotka and Volterra proposed the predator-prey dynamic behavior model, many experts and scholars have studied various predator-prey models, which has laid a solid theoretical foundation for the latter study (see [4–6, 12, 16, 17, 21–24, 28–30]). This paper argues that beetles will gain certain benefits after successfully invading pine trees, and improves on the model proposed by Chen, changing the model from a competition model to a predator-prey model, considering that both pine trees and beetles can spread in space, thereby introducing a diffusion term, and establishing the following reaction-diffusion forest beetle outbreak model:

$$\begin{cases} \frac{\partial V(x,t)}{\partial t} = r_v V \left(1 - \frac{V}{K_v} - f_k \frac{B}{r+B} - P \frac{V}{K_v} M_v \right) + d_1 \Delta V, \\ \frac{\partial B(x,t)}{\partial t} = r_b B \left(1 - \frac{B}{K_e} \right) - \frac{\alpha(1-cM_v)B^2}{1+\beta B^2} - M_b P \frac{V}{K_v} M_v B + \xi V B + d_2 \Delta B, \\ V_x(0,t) = B_x(0,t) = 0, V_x(l\pi,t) = B_x(l\pi,t) = 0, \\ V(x,0) = V_0(x) \geq 0, B(x,0) = B_0(x) \geq 0, \\ x \in (0, l\pi), t > 0, \end{cases} \tag{1.3}$$

where $V(x,t)$ and $B(x,t)$ are the number of pine trees and the number of beetles at position x and time t respectively. $d_1 > 0$ and $d_2 > 0$ represent the diffusion coefficients of prey and predator respectively. $\xi > 0$ is the buff the beetles get, when the pine tree is attacked by beetles. The meanings of the remaining parameters are the same as those in (1.1) and (1.2), and will not be repeated here. The boundary condition is Neumann boundary condition and all parameters involved with the

model are positive. In order to simplify system (1.3), we denote $\tilde{t} = d_2 t$, $\tilde{v} = \frac{V}{K_v}$, $\tilde{b} = \frac{B}{K_v}$, $r_1 = \frac{r_v}{d_2}$, $r_2 = \frac{r_b}{d_2}$, $\beta_1 = \beta K_e^2$, $K = f_k K_e$, $m_v = M_v P$, $m_b = \frac{M_b M_v P}{d_2}$, $\alpha_f = \frac{\alpha(1-cM_v)K_e}{d_2}$, $\eta = \frac{\xi K_v}{d_2}$ and $d = \frac{d_1}{d_2}$. After ignoring the superscript, model (1.3) can be rewritten as follows:

$$\begin{cases} \frac{\partial v(x,t)}{\partial t} = r_1 v \left(1 - v - \frac{Kb}{r+K_e b} - m_v v \right) + d\Delta v, & x \in (0, l\pi), t > 0, \\ \frac{\partial b(x,t)}{\partial t} = b \left(r_2(1-b) - \frac{\alpha_f b}{1+\beta_1 b^2} - (m_b - \eta)v \right) + \Delta b, & x \in (0, l\pi), t > 0, \\ v_x(0,t) = b_x(0,t) = 0, v_x(l\pi,t) = b_x(l\pi,t) = 0, & t > 0, \\ v(x,0) = v_0(x) \geq 0, b(x,0) = b_0(x) \geq 0, & x \in (0, l\pi). \end{cases} \tag{1.4}$$

The general content of this article is as follows. In Section 2, the existence of positive equilibrium points of the system and the local asymptotic stability at positive equilibrium points are discussed. In Section 3, the existence of Turing bifurcation, Hopf bifurcation and Turing-Hopf bifurcation are investigated respectively, and the normal forms for Turing-Hopf bifurcation are discussed. In Section 4, some numerical simulations are given. Finally, in Section 5, a short conclusion is given.

2. Stability analysis of equilibria

2.1. Existence of the positive equilibria

Now, we analyze the existence of the positive equilibrium point of system (1.4). The equilibrium of system (1.4) satisfies:

$$\begin{cases} r_1 v \left(1 - v - \frac{Kb}{r+K_e b} - m_v v \right) = 0, \\ b \left(r_2(1-b) - \frac{\alpha_f b}{1+\beta_1 b^2} - (m_b - \eta)v \right) = 0. \end{cases} \tag{2.1}$$

Since a positive equilibrium point is required, $v > 0$, $b > 0$. According to (2.1), we have

$$\begin{cases} v = \frac{r+(K_e-K)b}{(1+m_v)(r+K_e b)}, \\ c_1 b^4 + c_2 b^3 + c_3 b^2 + c_4 b + c_5 = 0, \end{cases} \tag{2.2}$$

where $c_1 = -\beta_1 K_e r_2(1+m_v) < 0$, $c_5 = (\eta - m_b + r_2 + m_v r_2)r$ and $K_e > K(0 < f_k < 1)$. According to the first equation in (2.2), if $b > 0$, we can get $v > 0$, and if $\eta > m_b$ holds, from the continuity of the function, we can get that there exist $c_5 > 0$ and $b_* > 0$. Therefore, the second equation in (2.2) holds. Since Turing bifurcation and Hopf bifurcation will not occur in system (1.4), when $\eta \leq m_b$, the following chapters of this paper consistently assume that $\eta > m_b$ holds. The specific proof will be given in Section 3. Thus, system (1.4) must have a positive equilibrium point (v_*, b_*) .

2.2. Stability analysis of (v_*, b_*)

Now, we analyze the stability analysis of (v_*, b_*) as did in [27]. Define the real-valued Sobolev space

$$\mathbf{X} := \{(v, b) \in [H^2(0, l\pi)]^2 : (v_x, b_x)|_{x=0, l\pi} = (0, 0)\},$$

and the complexification of \mathbf{X}

$$\mathbf{X}_{\mathbb{C}} := \mathbf{X} \oplus i\mathbf{X} = \{x_1 + ix_2 : x_1, x_2 \in \mathbf{X}\}.$$

The linearized system form of the system (1.4) at (v_*, b_*) is as follows:

$$\begin{pmatrix} v_t \\ b_t \end{pmatrix} = L(s) \begin{pmatrix} v \\ b \end{pmatrix} := \begin{pmatrix} d & 0 \\ 0 & 1 \end{pmatrix} \begin{pmatrix} \Delta v \\ \Delta b \end{pmatrix} + \begin{pmatrix} r_1 a_1 & r_1 a_2 \\ b_1 & b_2 \end{pmatrix} \begin{pmatrix} u \\ v \end{pmatrix},$$

where a_1, a_2, b_1 and b_2 are defined in (2.3). The linearization of system (1.4) at the equilibrium point (v_*, b_*) is as follows:

$$L(s) = \begin{pmatrix} d \frac{\partial^2}{\partial x^2} + r_1 a_1 & r_1 a_2 \\ b_1 & \frac{\partial^2}{\partial x^2} + b_2 \end{pmatrix}$$

with the domain $D_{L(s)} = \mathbf{X}_{\mathbb{C}}$, and

$$\begin{aligned} a_1 &= -(1 + m_v)v_* < 0, & a_2 &= -\frac{Krv_*}{(r+K_e b_*)^2} < 0, \\ b_1 &= -(m_b - \eta)b_*, & b_2 &= r_2(1 - 2b_*) - \frac{2\alpha_f b_*}{(1+\beta_1 b_*^2)^2} - (m_b - \eta)v_*. \end{aligned} \tag{2.3}$$

We know that the eigenvalue problem

$$-\varphi'' = \mu\varphi, \quad x \in (0, l\pi), \quad \varphi'(0) = \varphi'(l\pi) = 0$$

has eigenvalues $\mu_n = \frac{n^2}{l^2}$ ($n = 0, 1, \dots$) with corresponding eigenfunctions $\varphi_n(x) = \cos \frac{nx}{l}$. We can let

$$\begin{pmatrix} \phi \\ \psi \end{pmatrix} = \sum_{n=0}^{\infty} \begin{pmatrix} a_n \\ b_n \end{pmatrix} \cos \frac{nx}{l}$$

be an eigenfunction of $L(s)$ corresponding to an eigenvalue $\beta(s)$. Then we can get as follows:

$$L(s)(\phi, \psi)^T = \beta(s)(\phi, \psi)^T.$$

From a straightforward analysis, we have

$$L_n(s) \begin{pmatrix} a_n \\ b_n \end{pmatrix} = \beta(s) \begin{pmatrix} a_n \\ b_n \end{pmatrix}, \quad n = 0, 1, \dots,$$

where

$$L_n(s) := \begin{pmatrix} r_1 a_1 - d\mu_n & r_1 a_2 \\ b_1 & b_2 - \mu_n \end{pmatrix}.$$

The eigenvalues of $L(s)$ are given by the eigenvalues of $L_n(s)$ for $n = 0, 1, 2, \dots$, and the characteristic equation of $L_n(s)$ is as follows:

$$\lambda^2 - TR_n\lambda + DET_n = 0, \quad n = 0, 1, 2, \dots, \tag{2.4}$$

where

$$\begin{aligned} TR_n &= -(d+1)\mu_n + r_1a_1 + b_2, \\ DET_n &= d\mu_n^2 - (r_1a_1 + b_2d)\mu_n + r_1(a_1b_2 - a_2b_1). \end{aligned} \quad (2.5)$$

We can obtain the eigenvalues of (2.4) as follows:

$$\lambda_{1,2} = \frac{TR_n \pm \sqrt{TR_n^2 - 4DET_n}}{2}, \quad n = 0, 1, 2, 3, \dots$$

The following theorem can be obtained.

Theorem 2.1. *If $TR_n < 0$ and $DET_n > 0$ hold, then the real parts of the eigenvalues of system (1.4) are all less than zero, and system (1.4) is locally asymptotically stable at the positive equilibrium point (v_*, b_*) .*

3. Bifurcation analysis

We make the following assumptions:

$$\begin{aligned} (\mathbf{H}_1) &: r_1a_1 + b_2 < 0, r_1(a_1b_2 - a_2b_1) > 0; \\ (\mathbf{H}_2) &: r_1(a_1b_2 - a_2b_1) > 0, \end{aligned}$$

where (\mathbf{H}_1) determines the stability of the system without diffusion, and is a necessary condition for the system to generate Turing instability, while (\mathbf{H}_2) is a necessary condition for the system to generate Hopf bifurcation without diffusion. Both of them will be used in the subsequent system bifurcation analysis. In order to simplify the subsequent proof steps, these two assumptions are given here first.

3.1. Turing instability

According to [11, 25], for an equilibrium point that makes a system of ordinary differential equations stable, when a diffusion term is added to the system, it is no longer stable at the equilibrium point, and this phenomenon is called Turing instability.

Under assumption (\mathbf{H}_1) , we have $TR_n < TR_0 < 0$ and $DET_0 > 0$ for $n \in \mathbb{N}_0$. According to Theorem 2.1, the system of ordinary differential equations corresponding to system (1.4) is locally asymptotically stable at the positive equilibrium point (u^*, v^*) .

Now, we select d as the parameter of Turing bifurcation line. According to (2.5), we get an open-up quadratic function of μ : $DET(\mu) = d\mu^2 - (r_1a_1 + b_2d)\mu + r_1(a_1b_2 - a_2b_1)$ and $DET(0) = r_1(a_1b_2 - a_2b_1) > 0$. For $n \neq 0$, the symmetry axis μ_* and the discriminant Δ of $DET(\mu)$ are given as follows:

$$\mu_* = \frac{(r_1a_1 + b_2d)}{2d}, \quad \Delta = (r_1a_1 + b_2d)^2 - 4dr_1(a_1b_2 - a_2b_1).$$

There are two cases to be considered as follows:

Case I: $r_1a_1 + b_2d \leq 0$ or $\Delta < 0$. Then, all the roots of (2.4) have negative real parts.

Case II: $r_1a_1 + b_2d > 0$ and $\Delta > 0$. Denote the two different roots of $DET(\mu) = 0$ as μ_l and μ_r ($\mu_l < \mu_r$). By straightforward calculation, we have $\mu_{l,r} = \frac{(r_1a_1 + b_2d) \mp \sqrt{\Delta}}{2d}$, and get the following conclusions:

(i) For $\forall n \in \mathbb{N}$, if $\mu_n \notin (\mu_l, \mu_r)$, we have $DET(\mu_n) > 0$, and all the roots of (2.4) have negative real parts.

(ii) If there exists a $k \in \mathbb{N}$ such that $\mu_k \in (\mu_l, \mu_r)$ and $DET(\mu_k) < 0$, (2.4) will have at least one root with positive real part.

In summary, the following theorem can be obtained.

Theorem 3.1. *For system (1.4), we suppose (H_1) hold, and the following statements are true.*

- (1) *In Case I, system (1.4) is locally asymptotically stable at the positive equilibrium point (v_*, b_*) .*
- (2) *In Case II, $\mu_n \notin (\mu_l, \mu_r)$ for $\forall n \in \mathbb{N}$, and system (1.4) is locally asymptotically stable at the positive equilibrium point (v_*, b_*) .*
- (3) *In Case II, there exists a $k \in \mathbb{N}$ such that $\mu_k \in (\mu_l, \mu_r)$, and system (1.4) is Turing instability at the positive equilibrium point (v_*, b_*) .*

Furthermore, the case of $\eta \leq m_b$ is discussed. Under $\eta \leq m_b$ and assumptions (H_1) , we have $b_1 \leq 0, b_2 < 0, r_1 a_1 + b_2 d < 0$ in Case I. Therefore, system (1.4) will not have Turing instability phenomenon.

3.2. Hopf bifurcation

Hopf bifurcation refers to a phenomenon in nonlinear equations with parameters that reverses the stability of the trivial steady-state solution of the system with the change of the parameters, thereby generating a period near the trivial steady-state solution. If the system wants to have a Hopf bifurcation, its corresponding linearization operator needs to have a pair of pure imaginary eigenroots at the critical value, and satisfy the corresponding transversal conditions.

In this section, the parameter r_1 will be selected to study Hopf bifurcation in system (1.4).

Denote

$$r_1 = r_{1n} := \frac{(1 + d)\mu_n - b_2}{a_1}, n \in \mathbb{N}_0.$$

Under assumption (H_2) , we have $DET_0(r_{10}) > 0$.

Denote

$$n^* = \max\{ n \mid DET_n(r_{1n}) > 0, r_{1n} > 0, n \in \mathbb{N}\}.$$

When $r_1 = r_{1n}, 0 \leq n \leq n^*$, we have $TR_n(r_{1n}) = 0, DET_n(r_{1n}) > 0$, and system (1.4) has a pair of pure imaginary eigenvalues. We assume that system (1.4) has a pair of complex eigenvalues $\alpha_n(r_1) \pm i\omega_n(r_1)$ when r_1 is near r_{1n} , where

$$\alpha_n(r_1) = \frac{TR_n}{2}, \quad \omega_n(r_1) = \frac{\sqrt{4DET_n - TR_n^2}}{2}, \quad \left. \frac{d\alpha_n(r_1)}{dr_1} \right|_{r_1=r_{1n}} = \frac{a_1}{2} < 0.$$

The transversal condition is satisfied, and system (1.4) undergoes a Hopf bifurcation at $r_1 = r_{1n}$. Thus we can get the following theorem.

Theorem 3.2. *If (H_2) holds, system (1.4) undergoes a Hopf bifurcation at $r_1 = r_{1n}$, where $n = 0, 1, 2, \dots, n^*$.*

Furthermore, the case of $\eta \leq m_b$ is discussed. Under $\eta \leq m_b$ and assumption (H_2) , we have $b_1 \leq 0, b_2 < 0, T_n < 0$. System (1.4) will not have pure imaginary eigenvalues and Hopf bifurcation phenomenon.

3.3. Turing-Hopf bifurcation

Turing-Hopf bifurcation refers to the combination of Turing bifurcation and Hopf bifurcation, so that the system can generate Hopf bifurcation when there is no diffusion, and then generate Turing bifurcation after adding a diffusion.

If system (1.4) undergoes Turing-Hopf bifurcation, the following two conditions need to be satisfied:

- (i) When $n = 0$, equation (2.5) has a pair of pure imaginary roots.
- (ii) When $n > 0$, equation (2.5) has a single zero root.

In this section, we assume that (\mathbf{H}_2) always holds.

Denote

$$d_n = r_1 \left(\frac{a_1 \mu_n + a_2 b_1 - a_1 b_2}{\mu_n (\mu_n - b_2)} \right), S = \{ n \mid n \in \mathbb{N}, \mu_n - b_2 < 0 \},$$

such that

$$d_{n_*} = \min_{n \in S} \left\{ r_{10} \left(\frac{a_1 \mu_n + a_2 b_1 - a_1 b_2}{\mu_n (\mu_n - b_2)} \right) \right\}.$$

In r_1 - d plane, the Turing bifurcation curves are as follows:

$$\mathcal{L}_n : d_n = r_1 \left(\frac{a_1 \mu_n + a_2 b_1 - a_1 b_2}{\mu_n (\mu_n - b_2)} \right), n \in S,$$

and the Hopf bifurcation curve is as follows:

$$\mathcal{H}_0 : r_1 = r_{10}.$$

When $n = 0$, $r_1 = r_{10}$, system (1.4) undergoes Hopf bifurcation according to Theorem 3.2.

Now, we discuss the case of $n \neq 0$. If $S = \emptyset$, the Turing bifurcation curves \mathcal{L}_n and the Hopf bifurcation curve \mathcal{H}_0 have no intersection point in the first quadrant, and system (1.4) will not undergo Turing-Hopf bifurcation. If $S \neq \emptyset$, the Turing bifurcation curves \mathcal{L}_n and the Hopf bifurcation curve \mathcal{H}_0 have the intersection point (r_{10}, d_{n_*}) in the first quadrant, and the following cross-sectional conditions are obtained:

$$\begin{aligned} \left. \frac{dRe(\lambda)}{dr_1} \right|_{r_1=r_{10}, \mathcal{H}_0} &= \frac{a_1}{2} < 0, \\ \left. \frac{d\lambda}{dd} \right|_{d=d_{n_*}, \mathcal{L}_{n_*}} &= \frac{\mu_{n_*} (\mu_{n_*} - b_2)}{T_{n_*}} > 0. \end{aligned}$$

System (1.4) undergoes Turing-Hopf bifurcation at the point $(r_1, d) = (r_{10}, d_{n_*})$. In addition, when $(r_1, d) \in \{(r_1, d) \mid r_1 > r_{10}, 0 < d < d_{n_*}\}$, we have $TR_n < 0, DET_n > 0$, then the positive equilibrium point (v_*, b_*) is locally asymptotically stable. In summary, the following theorem can be obtained.

Theorem 3.3. *The following statements are true:*

- (1) If $S = \emptyset$, system (1.4) does not undergo Turing-Hopf bifurcation.
- (2) If $S \neq \emptyset$, system (1.4) undergoes Turing-Hopf bifurcation at the point $(r_1, d) = (r_{10}, d_{n_*})$, and when $(r_1, d) \in \{(r_1, d) \mid r_1 > r_{10}, 0 < d < d_{n_*}\}$, it is locally asymptotically stable at the positive equilibrium point (v_*, b_*) .

3.4. Normal forms for Turing-Hopf bifurcation

In this section, we calculate the normal forms to analyze the dynamic properties of system (1.4), when it undergoes Turing-Hopf bifurcation at the positive equilibrium point (v_*, b_*) . Some of the formulas can be referred to [10].

First, we define parameters δ_1, δ_2 , let $r_1 = r_{10} + \delta_1, d = d_{n_*} + \delta_2$ and transform system (1.4) into the following form:

$$\begin{cases} \frac{\partial v(x,t)}{\partial t} = (r_{10} + \delta_1)v \left(1 - v - \frac{Kb}{r+K_e b} - m_v v\right) + (d_{n_*} + \delta_2)\Delta v, \\ \frac{\partial b(x,t)}{\partial t} = b \left(r_2(1 - b) - \frac{\alpha_f b}{1+\beta_1 b^2} - (m_b - \eta)v\right) + \Delta b. \end{cases} \tag{3.1}$$

The equilibrium point of system (3.1) is still the positive equilibrium point (v_*, b_*) . Let $\bar{v} = v - v_*, \bar{b} = b - b_*$. After ignoring the horizontal bar, system (3.1) becomes the following system:

$$\begin{cases} \frac{\partial v(x,t)}{\partial t} = (r_{10} + \delta_1)(v + v_*) \left(1 - (v + v_*) - \frac{K(b+b_*)}{r+K_e(b+b_*)} - m_v(v + v_*)\right) \\ \quad + (d_{n_*} + \delta_2)\Delta v, \\ \frac{\partial b(x,t)}{\partial t} = (b + b_*) \left(r_2(1 - (b + b_*)) - \frac{\alpha_f(b+b_*)}{1+\beta_1(b+b_*)^2} - (m_b - \eta)(v + v_*)\right) \\ \quad + \Delta b. \end{cases} \tag{3.2}$$

According to [10], for system (3.2), we can get

$$D(\delta) = \begin{pmatrix} d_{n_*} + \delta_2 & 0 \\ 0 & 1 \end{pmatrix},$$

$$L(\delta) = \begin{pmatrix} (r_{10} + \delta_1)a_1 & (r_{10} + \delta_1)a_2 \\ b_1 & -r_{10}a_1 \end{pmatrix},$$

$$F(\phi, \delta) = \begin{pmatrix} (r_{10} + \delta_1)(\phi_1 + v_*) \left(1 - \frac{K(\phi_2+b_*)}{r+K_e(\phi_2+b_*)} - (m_v + 1)(\phi_1 + v_*)\right) \\ \quad - (r_{10} + \delta_1)(a_1\phi_1 + a_2\phi_2) \\ (\phi_2 + b_*) \left(r_2(1 - (\phi_2 + b_*)) - \frac{\alpha_f(\phi_2+b_*)}{1+\beta_1(\phi_2+b_*)^2} - (m_b - \eta)(\phi_1 + v_*)\right) \\ \quad - b_1\phi_1 + r_{10}a_1\phi_2 \end{pmatrix},$$

where $\phi = (\phi_1, \phi_2)^T \in X$, then we have

$$D(0) = \begin{pmatrix} d_{n_*} & 0 \\ 0 & 1 \end{pmatrix}, \quad D_1(\delta) = \begin{pmatrix} 2\delta_2 & 0 \\ 0 & 0 \end{pmatrix},$$

$$L(0) = \begin{pmatrix} r_{10}a_1 & r_{10}a_2 \\ b_1 & -r_{10}a_1 \end{pmatrix}, \quad L_1(\delta) = \begin{pmatrix} 2\delta_1a_1 & 2\delta_1a_2 \\ 0 & 0 \end{pmatrix},$$

$$Q(\phi, \psi) = \begin{pmatrix} \alpha_{11}\phi_1\psi_1 + \alpha_{12}(\phi_1\psi_2 + \phi_2\psi_1) + \alpha_{13}\phi_2\psi_2 \\ \alpha_{21}\phi_1\psi_1 + \alpha_{22}(\phi_1\psi_2 + \phi_2\psi_1) + \alpha_{23}\phi_2\psi_2 \end{pmatrix},$$

$$C(\phi, \psi, v) = \begin{pmatrix} \beta_{11}\phi_1\psi_1v_1 + \beta_{12}(\phi_1\psi_1v_2 + \phi_1\psi_2v_1 + \phi_2\psi_1v_1) \\ +\beta_{13}(\phi_2\psi_2v_1 + \phi_2\psi_1v_2 + \phi_1\psi_2v_2) + \beta_{14}\phi_2\psi_2v_2 \\ \beta_{21}\phi_1\psi_1v_1 + \beta_{22}(\phi_1\psi_1v_2 + \phi_1\psi_2v_1 + \phi_2\psi_1v_1) \\ +\beta_{23}(\phi_2\psi_2v_1 + \phi_2\psi_1v_2 + \phi_1\psi_2v_2) + \beta_{24}\phi_2\psi_2v_2 \end{pmatrix},$$

where

$$\begin{aligned} \alpha_{11} &= -(1 + m_v)r_{10}, \alpha_{12} = -\frac{Krr_{10}}{2(b_*K_e+r)^2}, \alpha_{13} = \frac{KK_e r r_{10} v_*}{(b_*K_e+r)^3}, \\ \alpha_{22} &= \frac{-m_b+\eta}{2}, \alpha_{23} = \frac{\alpha_f - 3\alpha_f b_*^2 \beta_1 + (1+b_*^2 \beta_1)^3 r_2}{(1+b_*^2 \beta_1)^3}, \\ \beta_{13} &= \frac{KK_e r r_{10}}{3(b_*K_e+r)^3}, \beta_{14} = -\frac{KK_e^2 r r_{10} v_*}{(b_*K_e+r)^4}, \beta_{24} = -\frac{4\alpha_f b_* \beta_1 (-1+b_*^2 \beta_1)}{(1+b_*^2 \beta_1)^4}, \\ \alpha_{21} &= \beta_{11} = \beta_{12} = \beta_{21} = \beta_{22} = \beta_{23} = 0. \end{aligned}$$

The characteristic matrix corresponding to the system (3.2) is as follows:

$$D_n(\lambda) = \begin{pmatrix} \lambda + d_{n_*} \mu_n - r_{10} a_1 & -r_{10} a_2 \\ -b_1 & \lambda + \mu_n + r_{10} a_1 \end{pmatrix}.$$

According to Theorem 3.3, $\lambda = \pm i\omega$ with $\omega = \sqrt{DET_0}$ is a pair of pure imaginary eigenvalues of $D_0(\lambda)$. $\lambda = 0$ is the single zero eigenvalue of $D_{n_*}(\lambda)$. We can obtain the following:

$$\phi_1 = \begin{pmatrix} 1 \\ \frac{d_{n_*} \mu_{n_*} - r_{10} a_1}{r_{10} a_2} \end{pmatrix}, \psi_1 = \begin{pmatrix} \frac{r_{10} a_2 b_1}{(d_{n_*} \mu_{n_*} - r_{10} a_1)^2 + r_{10} a_2 b_1} \\ \frac{r_{10} a_2 (d_{n_*} \mu_{n_*} - r_{10} a_1)}{(d_{n_*} \mu_{n_*} - r_{10} a_1)^2 + r_{10} a_2 b_1} \end{pmatrix}^T,$$

$$\phi_2 = \begin{pmatrix} 1 \\ \frac{i\omega - r_{10} a_1}{r_{10} a_2} \end{pmatrix}, \psi_2 = \begin{pmatrix} \frac{r_{10} a_2 b_1}{(i\omega - r_{10} a_1)^2 + r_{10} a_2 b_1} \\ \frac{r_{10} a_2 (i\omega - r_{10} a_1)}{(i\omega - r_{10} a_1)^2 + r_{10} a_2 b_1} \end{pmatrix}^T,$$

where $\Phi = (\phi_1, \phi_2, \bar{\phi}_2)$, $\Psi = (\psi_1, \psi_2, \bar{\psi}_2)$, $\Psi\Phi = I_3$, and I_3 is the identity matrix. In

addition, the following parameters are given:

$$\begin{aligned}
 a_1(\delta) &= \frac{1}{2}\psi_1(L_1(\delta)\phi_1 - \mu_{n_*}D_1(\delta)\phi_1), \\
 a_{200} &= a_{011} = b_{110} = 0, \\
 b_2(\delta) &= \frac{1}{2}\psi_2(L_1(\delta)\phi_2 - 0D_1(\delta)\phi_2), \\
 a_{300} &= \frac{1}{4}\psi_1C_{\phi_1\phi_1\phi_1} + \frac{1}{\omega}\psi_1Re[iQ_{\phi_1\phi_2}\psi_2]Q_{\phi_1\phi_1} + \psi_1Q_{\phi_1(h_{200}^0 + \frac{1}{\sqrt{2}}h_{200}^{2n_*})}, \\
 a_{111} &= \psi_1C_{\phi_1\phi_2\bar{\phi}_2} + \frac{2}{\omega}\psi_1Re[iQ_{\phi_1\phi_2}\psi_2]Q_{\phi_2\bar{\phi}_2} + \psi_1(Q_{\phi_1(h_{011}^0 + \frac{1}{\sqrt{2}}h_{011}^{2n_*})} + Q_{\phi_2h_{101}^{n_*}} \\
 &\quad + Q_{\bar{\phi}_2h_{110}^{n_*}}), \\
 b_{210} &= \frac{1}{2}\psi_2C_{\phi_1\phi_1\phi_2} + \frac{1}{2i\omega}\psi_2(2Q_{\phi_1\phi_1}\psi_1Q_{\phi_1\phi_2} + (-Q_{\phi_2\phi_2}\psi_2 + Q_{\phi_2\bar{\phi}_2}\bar{\psi}_2)Q_{\phi_1\phi_1}) \\
 &\quad + \psi_2(Q_{\phi_1h_{110}^{n_*}} + Q_{\phi_2h_{200}^0}), \\
 b_{021} &= \frac{1}{2}\psi_2C_{\phi_2\phi_2\bar{\phi}_2} + \frac{1}{4i\omega}\psi_2\left(\frac{2}{3}Q_{\bar{\phi}_2\bar{\phi}_2}\bar{\psi}_2Q_{\phi_2\phi_2} + (-2Q_{\phi_2\phi_2}\psi_2 + 4Q_{\phi_2\bar{\phi}_2}\bar{\psi}_2)Q_{\phi_2\bar{\phi}_2}\right) \\
 &\quad + \psi_2(Q_{\phi_2h_{011}^0} + Q_{\bar{\phi}_2h_{020}^0}), \\
 h_{200}^0 &= -\frac{1}{2}L^{-1}(0)Q_{\phi_1\phi_1} + \frac{1}{2\omega i}(\phi_2\psi_2 - \bar{\phi}_2\bar{\psi}_2)Q_{\phi_1\phi_1}, \\
 h_{200}^{2n_*} &= -\frac{1}{2\sqrt{2}}[L(0) - 4\mu_{n_*}D(0)]^{-1}Q_{\phi_1\phi_1}, \\
 h_{011}^0 &= -L^{-1}(0)Q_{\phi_2\bar{\phi}_2} + \frac{1}{\omega i}(\phi_2\psi_2 - \bar{\phi}_2\bar{\psi}_2)Q_{\phi_2\bar{\phi}_2}, \\
 h_{020}^0 &= \frac{1}{2}[2i\omega I - L(0)]^{-1}Q_{\phi_2\phi_2} - \frac{1}{2\omega i}\left(\phi_2\psi_2 + \frac{1}{3}\bar{\phi}_2\bar{\psi}_2\right)Q_{\phi_2\phi_2}, \\
 h_{110}^{n_*} &= [i\omega I - (L(0) - \text{diag}(-\mu_{n_*}, -d_{n_*}\mu_{n_*}))]^{-1}Q_{\phi_1\phi_2} - \frac{1}{\omega i}\phi_1\psi_1Q_{\phi_1\phi_2}, \\
 h_{002}^0 &= \bar{h}_{020}^0, h_{101}^{n_*} = \bar{h}_{110}^{n_*}, h_{011}^{2n_*} = 0.
 \end{aligned}$$

Thus, the normal form of system (1.4) is obtained at the Turing-Hopf bifurcation as follows:

$$\begin{cases} \dot{z}_1 = a_1(\delta)z_1 + a_{200}z_1^2 + a_{011}z_2\bar{z}_2 + a_{300}z_1^3 + a_{111}z_1z_2\bar{z}_2 + h.o.t., \\ \dot{z}_2 = i\omega z_2 + b_2(\delta)z_2 + b_{110}z_1z_2 + b_{210}z_1^2z_2 + b_{021}z_2^2\bar{z}_2 + h.o.t., \\ \dot{\bar{z}}_2 = -i\omega\bar{z}_2 + \bar{b}_2(\delta)\bar{z}_2 + \bar{b}_{110}z_1\bar{z}_2 + \bar{b}_{210}z_1^2\bar{z}_2 + \bar{b}_{021}z_2\bar{z}_2^2 + h.o.t.. \end{cases} \tag{3.3}$$

Let $z_1 = r$, $z_2 = \rho \cos\theta - \rho i \sin\theta$, and convert system (3.3) to cylindrical coordinate form:

$$\begin{cases} \dot{r} = a_1(\delta)r + a_{300}r^3 + a_{111}r\rho^2, \\ \dot{\rho} = Re(b_2(\delta))\rho + Re(b_{210})\rho r^2 + Re(b_{021})\rho^3. \end{cases} \tag{3.4}$$

4. Numerical simulations

In this section, simulations were performed to verify the previous conclusions. Let $r_2 = 0.16$, $K = 1$, $K_e = 3$, $r = 1$, $\beta_1 = 4$, $\alpha_f = 1.5$, $m_v = 1.5$, $m_b = 3$, $\eta =$

4 and $l = 100$, system (1.4) becomes as follows:

$$\begin{cases} \frac{\partial v(x,t)}{\partial t} = r_1 v \left(1 - v - \frac{b}{1+3b} - 1.5v \right) + d\Delta v, \\ \frac{\partial b(x,t)}{\partial t} = b \left(0.16(1 - b) - \frac{1.5b}{1+4b^2} + v \right) + \Delta b. \end{cases} \quad (4.1)$$

After computation, system (4.1) has a unique equilibrium point $(v_*, b_*) = (0.3, 1)$, and assumption (\mathbf{H}_2) is verified. Calculating other parameter values under this condition, $a_1 = -0.75$, $a_2 = -0.01875$, $b_1 = 1$ and $b_2 = 0.02$. In r_1 - d plane, the Hopf bifurcation curve is as follows:

$$\mathcal{H}_0 : r_1 = r_{10} \approx 0.026667,$$

and the Turing bifurcation curves are as follows:

$$\mathcal{L}_n : d_n = r_1 \left(\frac{a_1 \mu_n + a_2 b_1 - a_1 b_2}{\mu_n (\mu_n - b_2)} \right), n \in S = \{1, 2, 3, \dots, 13, 14\}.$$

The Turing bifurcation curves \mathcal{L}_n and the Hopf bifurcation curve \mathcal{H}_0 have the first intersection point $(r_{10}, d_{n_*}) \approx (0.026667, 2.61949)$ in the first quadrant (see Figure 1).

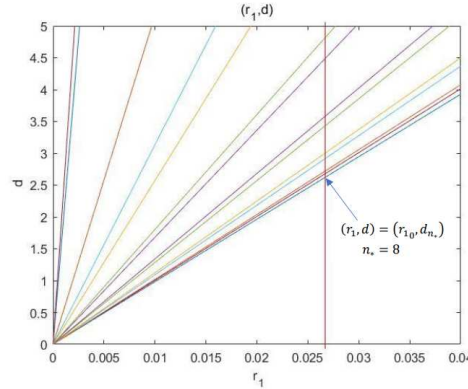


Figure 1. When $n_* = 8$, we have the first intersection of the Turing bifurcation curves \mathcal{L}_n and the Hopf bifurcation curve \mathcal{H}_0 at the point $(r_{10}, d_{n_*}) \approx (0.026667, 2.61949)$.

The normal form of system (4.1) is as follows:

$$\begin{cases} \dot{z}_1 = -0.369096(\delta_1 - 0.0101801\delta_2)z_1 + 437.822z_1^3 - 83.0370z_1z_2\bar{z}_2 \\ \quad + h.o.t., \\ \dot{z}_2 = 0.01iz_2 - (0.375 - 0.1875i)\delta_1z_2 - (566.464 + 245.969i)z_1^2z_2 \\ \quad - (9.6375 + 106.401i)z_2^2\bar{z}_2 + h.o.t., \\ \dot{\bar{z}}_2 = -0.01i\bar{z}_2 - (0.375 + 0.1875i)\delta_1\bar{z}_2 - (566.464 - 245.969i)z_1^2\bar{z}_2 \\ \quad - (9.6375 - 106.401i)z_2\bar{z}_2^2 + h.o.t.. \end{cases} \quad (4.2)$$

We get its cylindrical coordinate form as follows:

$$\begin{cases} \dot{r} = -0.369096(\delta_1 - 0.0101801\delta_2)r + 437.822r^3 - 83.0370r\rho^2, \\ \dot{\rho} = -0.375\delta_1\rho - 566.464\rho r^2 - 9.63750\rho^3. \end{cases} \quad (4.3)$$

Considering $\rho > 0$, system (4.3) has the following equilibrium:

- (1) The coexistence equilibrium: $A_0 = (0, 0)$.
- (2) Spatially inhomogeneous steady states:

$$A_1^\pm = (\pm 0.0000888142\sqrt{106875\delta_1 - 1088\delta_2}, 0), \text{ for } 106875\delta_1 - 1088\delta_2 > 0.$$

- (3) Spatially homogeneous periodic solution:

$$A_2 = (0, 0.197257\sqrt{-\delta_1}), \text{ for } \delta_1 < 0.$$

- (4) Spatially inhomogeneous periodic solutions:

$$A_3^\pm = (\pm\sigma_1, \sigma_2),$$

$$\sigma_1 = 9.505 \times 10^{-5}\sqrt{-5.957 \times 10^4\delta_1 - 78.21\delta_2},$$

$$\sigma_2 = 3.68 \times 10^{-3}\sqrt{-5.369 \times 10^2\delta_1 + 3.061\delta_2},$$

and $-5.957 \times 10^4\delta_1 - 78.21\delta_2 > 0$, $-5.369 \times 10^2\delta_1 + 3.061\delta_2 > 0$.

The following bifurcating lines are obtained:

$$\mathcal{H}_0 : \delta_1 = 0,$$

$$\mathcal{T} : \delta_2 = 98.23\delta_1,$$

$$\mathcal{T}_1 : \delta_2 = -761.7\delta_1, \delta_1 \leq 0,$$

$$\mathcal{T}_2 : \delta_2 = 175.4\delta_1, \delta_1 \leq 0.$$

The parameter space is divided into six regions as shown below:

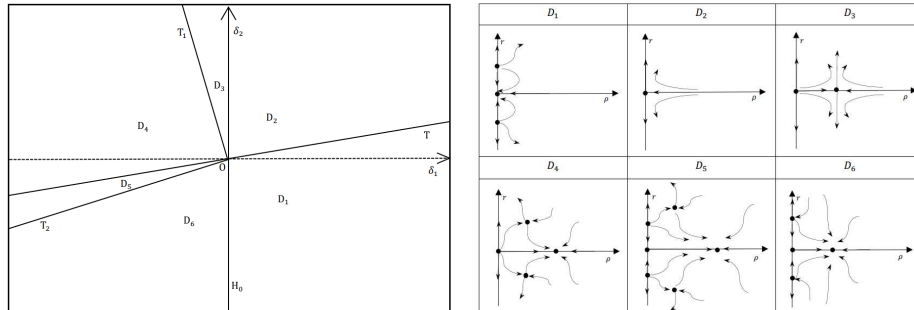


Figure 2. The bifurcation set and the phase portraits for Turing-Hopf bifurcation of system (4.1)

By analyzing the dynamic properties of each region, the following propositions can be obtained:

Proposition 4.1. *When $r_2 = 0.16, K = 1, K_e = 3, r = 1, \beta_1 = 4, \alpha_f = 1.5, m_v = 1.5, m_b = 3, \eta = 4, l = 100$, the parameter space is divided into six regions by branch lines $\mathcal{H}_0, \mathcal{T}, \mathcal{T}_1, \mathcal{T}_2$. System (1.4) has different dynamical phenomena occurring in these six regions.*

- (1) When $(\delta_1, \delta_2) \in D_1$, system (1.4) has a locally asymptotically stable positive equilibrium point and a pair of unstable spatially inhomogeneous steady states, and the pair of unstable spatially inhomogeneous steady states is attracted to the locally asymptotically stable positive equilibrium point. The numbers of pine trees and beetles are stable at the equilibrium point, thus pines and beetles coexist (See Figure 3).
- (2) When $(\delta_1, \delta_2) \in D_2$, system (1.4) has an unstable positive equilibrium point. The numbers of pines and beetles are both unstable at the equilibrium point.
- (3) When $(\delta_1, \delta_2) \in D_3$, system (1.4) has an unstable positive equilibrium point and an unstable spatially homogeneous periodic solution. The numbers of pines and beetles are still both unstable at the equilibrium point.
- (4) When $(\delta_1, \delta_2) \in D_4$, system (1.4) has a stable spatially homogeneous periodic, an unstable positive equilibrium point and a pair of unstable spatially inhomogeneous periodic solutions. The pair of unstable spatially inhomogeneous periodic solutions is attracted to the stable spatially homogeneous periodic. The population of pine trees and beetles fluctuates periodically over time (See Figure 4).
- (5) When $(\delta_1, \delta_2) \in D_5$, system (1.4) has a stable spatially homogeneous periodic, an unstable positive equilibrium point, a pair of unstable spatially inhomogeneous periodic solutions and a pair of unstable spatially inhomogeneous steady state. The pair of unstable spatially inhomogeneous periodic solutions and the pair of unstable spatially inhomogeneous steady states are attracted to the stable spatially homogeneous periodic. Finally, both pine and beetle population fluctuate periodically over time. Meanwhile, pines and beetles coexist and exhibit an oscillatory behavior (See Figure 5).
- (6) When $(\delta_1, \delta_2) \in D_6$, system (1.4) has a stable spatially homogeneous periodic, an unstable positive equilibrium point and a pair of unstable spatially inhomogeneous steady state. The pair of unstable spatially inhomogeneous steady states is attracted to the stable spatially homogeneous periodic. Pines and beetles coexist and still exhibit an oscillatory behavior (See Figure 6).

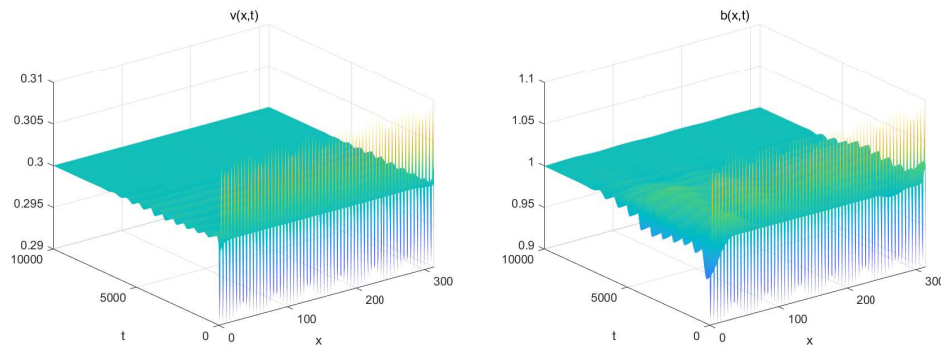


Figure 3. $(\delta_1, \delta_2) = (0.001, 0.05) \in D_1$, A_0 is locally asymptotically stable and A_1^\pm is unstable.

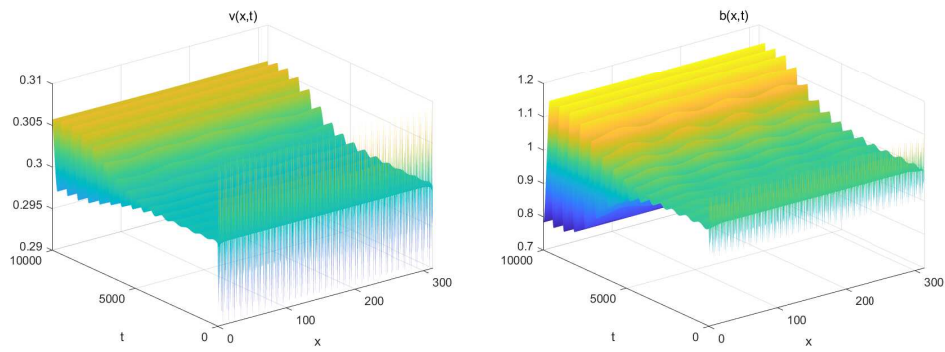


Figure 4. $(\delta_1, \delta_2) = (-0.001, -0.04) \in D_4$, A_2 is stable, while A_0 and A_3^\pm are unstable.

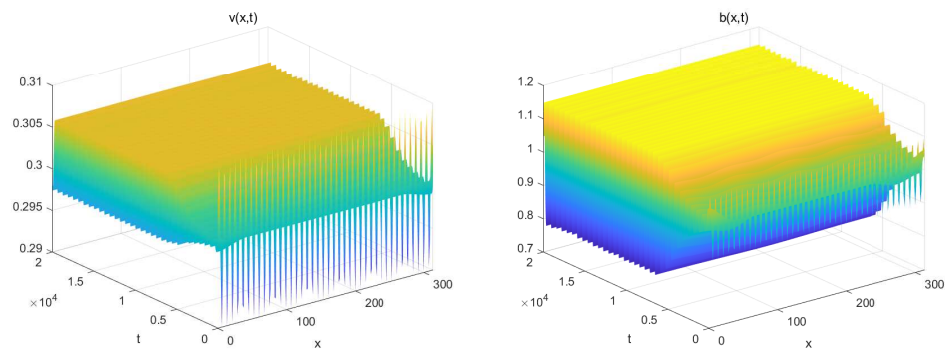


Figure 5. $(\delta_1, \delta_2) = (-0.001, -0.12) \in D_5$, A_2 is stable, while A_0, A_1^\pm and A_3^\pm are unstable.

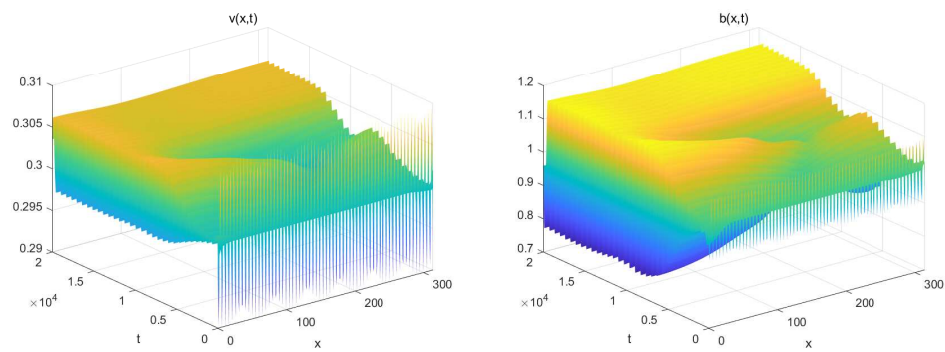


Figure 6. $(\delta_1, \delta_2) = (-0.001, -0.35) \in D_6$, A_2 is stable while A_0 and A_1^\pm are unstable.

Here, $v(x, 0) = 0.3 + 0.01\sin(5x)$ and $b(x, 0) = 1 + 0.1\sin(5x)$.

5. Conclusion

The diffusion phenomenon exists widely in nature. Based on the work of Chen, this paper analyzes the forest fire and forest beetle outbreak model with a diffusion term, and mainly carries out some bifurcation analyses on the local area of the positive equilibrium point.

This paper discusses the existence and stability of the positive equilibrium point of system (1.4), selects d and r_1 as the parameters of the Turing and Hopf bifurcations and obtains the necessary conditions for the existence of Turing instability, Hopf bifurcation and Turing-Hopf bifurcation respectively. By calculating the normal form of system (1.4) at the Turing-hopf bifurcation point, the parameter space is divided into six areas, and it is found that it is locally asymptotically stable at the positive equilibrium point of $D1$, where pine trees and beetles coexist, and system (1.4) is unstable at the positive equilibrium point of $D2, D3$, stable spatially homogeneous periodic solutions are generated at $D4, D5, D6$, where pines and beetles coexist and exhibit an oscillatory behavior.

Acknowledgements

The authors thank the reviewers and editors for their valuable suggestions that have helped improve this paper.

References

- [1] B. Beckage, L. J. Gross and W. J. Platt, *Grass feedbacks on fire stabilize savannas*, Ecological Modelling, 2011, 222(14), 2227–2233.
- [2] P. H. W. Biedermann, J. Müller, J. C. Grégoire, et al., *Bark beetle population dynamics in the anthropocene: challenges and solutions*, Trends in Ecology & Evolution, 2019, 34(10), 914–924.
- [3] B. Chen, *A model for coupling fire and insect outbreak in forests*, Ecological Modelling, 2014, 286(1), 26–36.
- [4] S. Chen, J. Wei and J. Yu, *Stationary patterns of a diffusive predator-prey model with Crowley-Martin functional response*, Nonlinear Analysis: Real World Applications, 2018, 39, 33–57.
- [5] H. Cheng, F. Wang and T. Zhang, *Multi-state dependent impulsive control for Holling I predator-prey model*, Discrete Dynamics in Nature and Society, 2012, 12, Article ID 181752, 21 pages.
- [6] H. Cheng, T. Zhang and F. Wang, *Existence and attractiveness of order one periodic solution of a Holling I predator-prey model*, Abstract and Applied Analysis, 2012, Article ID 126018, 18 pages.
- [7] C. M. Elkin and M. L. Reid, *Attack and reproductive success of mountain pine beetles (Coleoptera: Scolytidae) in Fire-Damaged Lodgepole Pines*, Environmental Entomology, 2004, 33(4), 1070–1080.
- [8] J. A. Hicke, M. C. Johnson, J. L. Hayes and H. K. Preisler, *Effects of bark beetle-caused tree mortality on wildfire*, Forest Ecology and Management, 2012, 271, 81–90.

- [9] C. S. Holling, *The components of predation as revealed by a study of small-mammal predation of the European pine sawfly*, Canadian Entomologist, 1959, 91(5), 293–320.
- [10] W. Jiang, Q. An and J. Shi, *Formulation of the normal form of Turing–Hopf bifurcation in partial functional differential equations*, Journal of Differential Equations, 2020, 268(10), 6067–6102.
- [11] W. Jiang, H. Wang and X. Cao, *Turing Instability and Turing–Hopf Bifurcation in Diffusive Schnakenberg Systems with Gene Expression Time Delay*, Journal of Dynamics and Differential Equations, 2019, 31(4), 2223–2247.
- [12] Z. Ling, L. Zhang, M. Zhu and M. Banerjee, *Dynamical behaviour of a generalist predator-prey model with free boundary*, Boundary Value Problems, 2017, 139, 20 pages.
- [13] S. Liu, B. B. Lamberty, J. A. Hicke, et al., *Simulating the impacts of disturbances on forest carbon cycling in north america: processes, data, models, and challenges*, Journal of Geophysical Research, 2011, 116, G00K08, 22 pages.
- [14] D. Ludwig, D. D. Jones and C. S. Holling, *Qualitative Analysis of Insect Outbreak Systems: The Spruce Budworm and Forest*, Journal of Animal Ecology, 1978, 47(1), 315–332.
- [15] W. D. Mawby, F. P. Hain and C. A. Doggett, *Endemic and epidemic populations of southern pine beetle: implications of the two-phase model for forest managers*, Forest Science, 1989, 35(4), 1075–1087.
- [16] X. Meng and X. Wang, *Stochastic Predator-Prey System Subject to Lévy Jumps*, Discrete Dynamics in Nature and Society, 2016, Article ID 5749892, 13 pages.
- [17] X. Meng, S. Zhao and W. Zhang, *Adaptive dynamics analysis of a predator-prey model with selective disturbance*, Applied Mathematics and Computation, 2015, 266, 946–958.
- [18] K. F. Raffa and A. A. Berryman, *A mechanistic computer model of mountain pine beetle populations interacting with lodgepole pine stands and its implications for forest managers*, Forest Science, 1986, 32(3), 789–805.
- [19] A. T. Rohde and D. S. Pillod, *Spatiotemporal dynamics of insect pollinator communities in sagebrush steppe associated with weather and vegetation*, Global Ecology and Conservation, 2021, 29, e01691, 16 pages.
- [20] M. Simard, W. H. Romme, J. M. Griffin, et al., *Do mountain pine beetle outbreaks change the probability of active crown fire in lodgepole pine forests?*, Ecological Monographs, 2011, 81(1), 3–24.
- [21] J. Song, M. Hu, Y. Bai and Y. Xia, *Dynamic Analysis of a Non-autonomous Ratio-dependent Predator-prey Model with Additional Food*, Journal of Applied Analysis and Computation, 2018, 8(6), 1893–1909.
- [22] Y. Song, H. Jiang and Y. Yuan, *Turing-hopf Bifurcation in the Reaction-diffusion System with Delay and Application to a Diffusive Predator-prey Model*, Journal of Applied Analysis and Computation, 2019, 9(3), 1132–1164.
- [23] J. Wang, H. Cheng, Y. Li and X. Zhang, *The Geometrical Analysis of a Predator-prey Model with Multi-state Dependent Impulses*, Journal of Applied Analysis and Computation, 2018, 8(2), 427–442.

- [24] J. Wang, H. Cheng, X. Meng and B. G. S. A. Pradeep, *Geometrical analysis and control optimization of a predator–prey model with multi state-dependent impulse*, *Advances in Difference Equations*, 2017, 252, 17 pages.
- [25] J. Wang and S. Liu, *Turing and Hopf Bifurcation in a Diffusive Tumor-immune Model*, *Journal of Nonlinear Modeling and Analysis*, 2021, 3(3), 477–493.
- [26] G. Wells, *Bark Beetles and Fire: Two Forces of Nature Transforming Western Forests*, *Fire Science Digests*, 2012, 12, 15 pages.
- [27] F. Yi, J. Wei and J. Shi, *Bifurcation and spatiotemporal patterns in a homogeneous diffusive predator–prey system*, *Journal of Differential Equations*, 2009, 246(5), 1944–1977.
- [28] S. Zhang, X. Meng, T. Feng and T. Zhang, *Dynamics analysis and numerical simulations of a stochastic non-autonomous predator–prey system with impulsive effects*, *Nonlinear Analysis: Hybrid Systems*, 2017, 26, 19–37.
- [29] T. Zhang, X. Meng, Y. Song and T. Zhang, *A Stage-Structured Predator-Prey SI Model with Disease in the Prey and Impulsive Effects*, *Mathematical Modelling and Analysis*, 2013, 18(4), 505–528.
- [30] X. Zhang and H. Zhu, *Dynamics and pattern formation in homogeneous diffusive predator–prey systems with predator interference or foraging facilitation*, *Nonlinear Analysis: Real World Applications*, 2019, 48, 267–287.